

This discussion paper is/has been under review for the journal The Cryosphere (TC).
Please refer to the corresponding final paper in TC if available.

Arctic sea ice melt onset from passive microwave satellite data: 1979–2012

A. C. Bliss and M. R. Anderson

Department of Earth and Atmospheric Sciences, University of Nebraska-Lincoln, Lincoln, Nebraska, USA

Received: 14 May 2014 – Accepted: 16 May 2014 – Published: 6 June 2014

Correspondence to: A. C. Bliss (acbliss3@huskers.unl.edu)

Published by Copernicus Publications on behalf of the European Geosciences Union.

Arctic sea ice melt onset from passive microwave satellite data: 1979–2012

A. C. Bliss and
M. R. Anderson

Title Page

Abstract

Introduction

Conclusions

References

Tables

Figures

◀

▶

◀

▶

Back

Close

Full Screen / Esc

Printer-friendly Version

Interactive Discussion

Abstract

An updated version of the Snow Melt Onset Over Arctic Sea Ice from SMMR and SSM/I-SSMIS Brightness Temperatures is now available. The data record has been re-processed and extended to cover the years 1979–2012. From this data set, a statistical summary of melt onset (MO) dates on Arctic sea ice is presented. The mean MO date for the Arctic Region is 13 May (132.5 DOY) with a standard deviation of ± 7.3 days. Regionally, mean MO dates vary from 15 March (73.2 DOY) in the St. Lawrence Gulf to 10 June (160.9 DOY) in the Central Arctic. Statistically significant decadal trends indicate that MO is occurring 6.6 days decade⁻¹ earlier in the year for the Arctic Region. Regionally, MO trends are as great as -11.8 days decade⁻¹ in the East Siberian Sea. The Bering Sea is an outlier and MO is occurring 3.1 days decade⁻¹ later in the year.

1 Introduction

Changes in all aspects of the Arctic cryosphere observed by satellite since late 1978 have been dramatic over the last few decades. Record low annual sea ice extent minima were recorded numerous times in the last decade, most recently in September 2012 (Parkinson and Comiso, 2013). Sea ice is becoming increasingly young and thin (Maslanik et al., 2007, 2011; Kwok et al., 2009) and thus, is more susceptible to melting throughout the spring and summer months (Ngheim et al., 2007; Lindsay et al., 2009). The melt season is lengthening through changes in timing of the onset of melt in the spring and also by delaying the timing of freeze-up in the fall (Belchansky et al., 2004; Stroeve et al., 2006, 2014; Markus et al., 2009). Lengthening melt seasons increase ice volume loss in the Arctic, in particular, through earlier melt onset which strengthens the sea ice albedo feedback loop (Stroeve et al., 2006, 2014; Markus et al., 2009).

The albedo changes on the sea ice surface that occur when melt begins allow for the absorption of solar radiation, which then increases the amount of melting that occurs

TCD

8, 3037–3055, 2014

Arctic sea ice melt onset from passive microwave satellite data: 1979–2012

A. C. Bliss and
M. R. Anderson

Title Page

Abstract

Introduction

Conclusions

References

Tables

Figures

◀

▶

◀

▶

Back

Close

Full Screen / Esc

Printer-friendly Version

Interactive Discussion



Arctic sea ice melt onset from passive microwave satellite data: 1979–2012A. C. Bliss and
M. R. Anderson

Title Page

Abstract

Introduction

Conclusions

References

Tables

Figures

◀

▶

◀

▶

Back

Close

Full Screen / Esc

Printer-friendly Version

Interactive Discussion



within the ice–ocean system (Curry et al., 1995). An earlier date of melt onset on Arctic sea ice has a greater impact on the overall absorption of solar radiation in the ice–ocean system when compared to a lengthening of the melt season by a delay in the date of freeze-up in the fall (Perovich et al., 2007). Although no direct correlation between the melt onset date and September sea ice extent minima has been found (Wang et al., 2011), the date of melt onset in the Arctic signals the beginning of the melt season, and begins the ice-albedo feedbacks, which carry out through the remainder of the melt season (Stroeve et al., 2006; Markus et al., 2009).

Several algorithms exist to determine the date of melt onset on Arctic sea ice from passive microwave satellite observations (e.g. Smith, 1998; Drobot and Anderson, 2001; Belchansky et al., 2004; Markus et al., 2009) and also from active microwave satellite observations (e.g. Winebrenner et al., 1994; Forster et al., 2001; Kwok et al., 2003). However, melt onset dates from passive microwave observations are largely consistent for a longer time period (1979–present) than active microwave products.

We announce the release of the Snow Melt Onset Over Arctic Sea Ice from SMMR and SSM/I-SSMIS Brightness Temperatures, Version 3 (V3) data set that is now available for download from the National Snow and Ice Data Center (NSIDC) (Anderson et al., 2014), replacing the Version 2 (V2) data set. The melt onset (MO) dates in this updated data set are calculated using the Advanced Horizontal Range Algorithm (AHRA) developed by Drobot and Anderson (2001). The data set gives an annual view of the day of year (DOY) on which MO occurred at each pixel location. The data are available at a 25 km² resolution and are formatted using NSIDC’s polar stereographic 304 × 448 pixel Northern Hemisphere grid. The data set has been reprocessed from passive microwave brightness temperatures (T_{bs}) to improve the consistency of data processing and extend the record of annual MO dates through the 2012 melt season. In this work, we use this new data set to provide an updated statistical summary of MO dates for the 1979–2012 record and determine regional trends in the timing of MO for sea ice in the Arctic.

2 The data set and methodology

2.1 AHRA melt onset date calculation

The AHRA described by Drobot and Anderson (2001) utilizes horizontally polarized, daily-averaged, Tbs from the 18/19 and 37 GHz channels. Tbs were obtained from the Scanning Multichannel Microwave Radiometer (SMMR) on board the NASA Nimbus-7 satellite platform and the series of Special Sensor Microwave Imagers (SSM/I) and the Special Sensor Microwave Imager and Sounder (SMMIS) from the Defense Meteorological Satellite Program's F8, F11, F13, and F17 platforms. SMMR Tbs were collected every second day, while SSM/I and SSMIS Tbs are available daily. Prior to the calculation of melt dates, the Tbs are corrected using linear regression coefficients determined from sensor overlap areas using DMSP F8 as the baseline sensor (Jezek et al., 1991; Abdalati et al., 1995; Stroeve et al., 1998; W. Meier, personal communication, October 2011).

Tbs increase when liquid water is introduced to the snowpack atop the sea ice. The AHRA method tracks the difference between the 19 GHz (18 GHz for SMMR Tbs) and 37 GHz horizontally polarized Tbs at a given point. If the difference is > 4.0 K it is assumed that wintertime conditions exist at the point. If the difference is < -10.0 K then liquid water is likely present in the snow pack, causing a greater increase in the 37 GHz channel relative to the 18/19 GHz channel, and the date is recorded as the day of melt onset. If the difference falls between -10.0 and 4.0 K the 10 days prior and 9 days following the date in question are tested. If the difference between Tbs during the periods prior to and following the day in question is > 7.5 K a melt onset date is assigned. If this value is < 7.5 K no melt date is determined and the algorithm continues to the next day. During this stage of the algorithm, a large difference between the values prior to and following the date indicates a pattern shift in the time series of Tbs, thus melt onset has occurred. The use of the time series window surrounding the day makes the AHRA insensitive to spurious Tbs and weather interference. See Drobot and Anderson (2001) for full details on the algorithm.

Arctic sea ice melt onset from passive microwave satellite data: 1979–2012

A. C. Bliss and
M. R. Anderson

Title Page

Abstract

Introduction

Conclusions

References

Tables

Figures

◀

▶

◀

▶

Back

Close

Full Screen / Esc

Printer-friendly Version

Interactive Discussion



2.2 Updates to the data set

For Version 3 of the data set, some changes to the processing were made in addition to updating the record of annual MO dates through the 2012 melt season. The previous version of the data set (V2) was masked to the climatology of locations where a MO date had been calculated for every year in the 20 year period 1979–1998. This climatology mask was static and determined the pixels for which a melt date was calculated every year. The new data set (V3) no longer uses a static mask; instead, the MO dates are calculated for locations determined to be sea ice covered at the beginning of each melt season. The melt dates in a given year are calculated for pixel locations where sea ice concentration is $\geq 50\%$ on one or both of the first two days with data in March. The concentration data used here are Goddard merged sea ice concentrations available as part of the NOAA/NSIDC Arctic Sea Ice Climate Data Record (Meier et al., 2013). The beginning of March is used to represent full sea ice extent, since early March roughly corresponds to the annual maximum Arctic sea ice extent (e.g. Parkinson and Comiso, 2013). The first two days of data in March are used to account for days on which sea ice concentrations may be missing. Tbs were collected every second day during SMMR years (1979–1987); therefore, the sea ice concentrations used to create the ice mask for the MO dates data set may include two days during 1–5 March.

Since the sea ice mask is no longer static, the sea ice locations (especially along the ice edge) that experience MO throughout the melt season change from year to year. The annual MO date maps for 1979 and 2012 in Fig. 1 illustrate the changing sea ice mask and serve as sample data from the V3 data set. Due to the differences in swath width between the SMMR and SSM/I-SSMIS sensors, the data gap surrounding the North Pole (the pole hole) changes in diameter; examples of this can be seen in Fig. 1. The V2 climatology mask eliminated the difference between pole hole diameter that occurs; however, the reduction in diameter increases the amount of sea ice area for which MO is calculated, thus, increasing usefulness of the data for users who may subset the time series. Additionally, V2 of the data set included a 2 pixel buffer that

TCD

8, 3037–3055, 2014

Arctic sea ice melt onset from passive microwave satellite data: 1979–2012

A. C. Bliss and
M. R. Anderson

Title Page

Abstract

Introduction

Conclusions

References

Tables

Figures

◀

▶

◀

▶

Back

Close

Full Screen / Esc

Printer-friendly Version

Interactive Discussion

eliminated coastal sea ice locations where possible uncertainties in the Tbs from land-ocean spillover can occur. Newer versions of the Tb data have now corrected for this spillover uncertainty (Cavalieri et al., 1999); therefore, the buffer is no longer used for V3.

As noted above, before MO is calculated, the Tbs are corrected to improve inter-sensor calibration using linear regression coefficients. Version 3 of the data set extends the record using Tbs from the DMSP F17 satellite for the years 2008–2012. To be consistent with the rest of the record, the F17 Tbs are also corrected back to F8 Tbs using regression coefficients provided by W. Meier (personal communication, October 2011). Additionally, an erroneous application of the regression correction between SSM/I sensors on the DMSP F11 and F13 platforms was found and corrected for V3.

2.3 Calculation of statistics

All statistics reported here are calculated from pixel locations where a MO date exists in all 34 years of the data record. The sea ice locations (indicated by color) in Fig. 2 show the MO date climatology mask used in the calculation of statistics. Pixel locations in white do not have a melt date for one or more years and are excluded. Statistics are calculated for all of the Arctic sea ice cover (hereafter called the Arctic Region) and for smaller sub-regions of the Arctic that are identified by differing colors in Fig. 2. The area (in km²) for each sub-region of the Arctic is not equal in this work because we restrict calculations of statistics to the MO date climatology mask and implicitly the sea ice extent. We then divide the Arctic into common geographic regions. The regional boundaries used here are the same as used by Meier et al. (2007) except we include sea ice locations within the Baltic Sea. These regional boundaries are also similar to those of other works including Markus et al. (2009) and Parkinson et al. (1999) except that the region mask used here divides regions within the Arctic Ocean into smaller seas. The sea ice area for each region (in km²) is presented in Table 1. The area for the Arctic Region is the area sum of all 15 sub-regions.

Arctic sea ice melt onset from passive microwave satellite data: 1979–2012

A. C. Bliss and
M. R. Anderson

Title Page

Abstract

Introduction

Conclusions

References

Tables

Figures

◀

▶

◀

▶

Back

Close

Full Screen / Esc

Printer-friendly Version

Interactive Discussion



Arctic sea ice melt onset from passive microwave satellite data: 1979–2012

A. C. Bliss and
M. R. Anderson

Title Page

Abstract

Introduction

Conclusions

References

Tables

Figures

◀

▶

◀

▶

Back

Close

Full Screen / Esc

Printer-friendly Version

Interactive Discussion



All maps of summary statistics including the earliest MO date, latest MO date, range of MO dates, mean and standard deviation are calculated from the time series of MO dates at each individual pixel for 1979–2012. Regional statistics presented in Table 1 are calculated from the annual mean MO dates in each region (provided in Supplement Table S1). The mean earliest MO and mean latest MO values presented in Table 1 represent the earliest and latest of the annual mean MO dates, rather than the absolute earliest and latest MO dates from the 34 year record that appear in Fig. 3a and b. Regional trends are calculated from the slope of the least squares linear regression best-fit line on the time series of annual mean MO dates.

3 Melt onset statistics 1979–2012

Mean MO dates for the Arctic Region during the 34 year data record vary highly across the extent of sea ice cover (Fig. 3); however, the mean date of MO for the Arctic Region is 13 May (132.5 DOY) with a standard deviation of ± 7.3 days (Table 1). In general, the mean MO dates occur earliest at sea ice locations along the periphery of the sea ice edge and in the southernmost locations such as the Sea of Okhotsk, Bering Sea, Hudson Bay, Gulf of St. Lawrence, Greenland Sea, Baltic Sea, and Barents Sea (Table 1, Fig. 3d). This indicates a general latitudinal dependence on the timing of MO; however, the standard deviation of MO dates can be large in portions of these early-melting regions. Regions with higher standard deviations in mean MO date have higher variability in MO timing from year to year. The regions with the highest standard deviations occur in parts of the Arctic Ocean, including: the Barents, Kara, Laptev, East Siberian, Chukchi, and Beaufort Seas with the greatest standard deviation (± 14.5 days) occurring in the East Siberian Sea (Table 1).

The earliest MO dates during 1979–2012 occur at the beginning of the melt season, in early March, for most of the peripheral regions of the sea ice area (Fig. 3a). For portions of the Central Arctic, Canadian Archipelago, and the northern portion of the Beaufort Sea, the earliest MO dates do not occur until mid-late May. The earliest MO

Arctic sea ice melt onset from passive microwave satellite data: 1979–2012

A. C. Bliss and
M. R. Anderson

Title Page

Abstract

Introduction

Conclusions

References

Tables

Figures

◀

▶

◀

▶

Back

Close

Full Screen / Esc

Printer-friendly Version

Interactive Discussion

dates in other portions of the sea ice within the Arctic Ocean occur in late March and early April (warm colors in Fig. 3a). The latest MO dates in the record for much of the sea ice regions within the Arctic Ocean occur during August, while the coastal regions of the Arctic Ocean typically have the latest MO dates near the end of May through June (Fig. 3b). Two distinct areas of the sea ice cover appear to have a small range (warm colors in Fig. 3c), (1) in the peripheral sea ice regions (including the Sea of Okhotsk, the Bering Sea, the Labrador Sea (in the Baffin Bay region), and the southern Barents Sea) and (2) the North American side of the Arctic including parts of the Central Arctic, the northern Beaufort Sea, and the Canadian Archipelago regions. The variability in MO dates described by both ranges and standard deviations for these locations is small; however, the timing of MO is distinctly different. In the southern, peripheral regions, where the sea ice is primarily composed of seasonal, first year ice, air temperatures warm to the melting point earlier in the year and early MO dates are observed. Conversely, sea ice in the Central Arctic is typically thicker, multiyear ice. Sea ice concentrations would tend to be higher in this area and air temperatures would warm later in the year than at southern locations, leading to the later mean MO dates observed.

The St. Lawrence Gulf and Baltic Sea regions have the earliest mean MO dates, occurring 15 March (73.2 DOY) and 20 March (78.8 DOY), respectively, although both areas are small ($0.1 \times 10^5 \text{ km}^2$ and $0.2 \times 10^5 \text{ km}^2$) (Table 1). Other regions with relatively early mean MO dates (Table 1) are the Bering Sea, 21 March (79.9 DOY); the Sea of Okhotsk, 22 March (80.8 DOY); and the Barents Sea, 4 April (93.9 DOY). However, it is important to note that the early-melting sea ice in the Barents Sea is located in the southern, coastal portion of the region, while the sea ice in the northern half of the Barents, adjacent to the Central Arctic region, melts at a later date (Fig. 3d). The other peripheral and southern regions including: Hudson Bay, Baffin Bay, and the Greenland Sea have a mean MO date which occurs in the latter half of April. The remaining regions are located within the Arctic Ocean and have mean MO dates that range from 11 May

(130.5 DOY) in the Kara Sea to 10 June (160.9 DOY) in the Central Arctic region (Table 1).

MO dates can vary widely from year to year in Arctic sub-regions depending on when the air temperatures in different regions reach the melting point. There is some latitudinal dependence on the timing as indicated by the general pattern of mean MO dates where earliest MO occurs along the ice edge and at southernmost regions (Fig. 3); however, higher standard deviations and larger mean ranges in some sub-regions such as the Barents, Kara, Laptev, East Siberian, and Chukchi Seas indicate that there is a good amount of year to year variability in the timing of MO at the regional scale. Although, on average, there is latitudinal dependence on timing of MO, springtime weather conditions and temperature anomalies are important for explaining the year to year variability in MO timing for much of the sea ice within the Arctic Ocean (Anderson and Drobot, 2001; Belchansky et al., 2004; Wang et al., 2011; Markus et al., 2009). Springtime weather conditions, including cyclonic activity, can have an influence on the air temperatures and the surface energy budget of the sea ice through the trapping of longwave heat when conditions are cloudy or through increased incoming shortwave radiation when conditions are cloud free and the sun rises in spring.

4 Trends in melt onset dates

Trends in the time series of annual mean MO dates indicate that MO is occurring earlier in the year for the majority of Arctic sea ice over the 1979–2012 data record (Fig. 4). For the Arctic Region, a statistically significant trend (99 % confidence level) of $-6.6 \text{ days decade}^{-1}$ exists, indicating that MO is occurring earlier in the year in recent years when compared to the earliest years of the data record. Statistically significant negative trends also exist for sub-regions of the Arctic Ocean including: the Barents, Kara, Laptev, East Siberian, Chukchi, and Beaufort Seas, and the Canadian Archipelago and the Central Arctic region (99 % confidence level). These trends range from $-4.6 \text{ days decade}^{-1}$ in the Canadian Archipelago to $-11.8 \text{ days decade}^{-1}$ in the

Arctic sea ice melt onset from passive microwave satellite data: 1979–2012

A. C. Bliss and
M. R. Anderson

Title Page

Abstract

Introduction

Conclusions

References

Tables

Figures

◀

▶

◀

▶

Back

Close

Full Screen / Esc

Printer-friendly Version

Interactive Discussion



Arctic sea ice melt onset from passive microwave satellite data: 1979–2012

A. C. Bliss and
M. R. Anderson

Title Page

Abstract

Introduction

Conclusions

References

Tables

Figures

◀

▶

◀

▶

Back

Close

Full Screen / Esc

Printer-friendly Version

Interactive Discussion

East Siberian Sea. R^2 values vary, but are strongest for the Arctic Region and the Central Arctic where the R^2 value is at least 0.76 (Fig. 4). Statistically significant trends also exist in the Bering Sea and Baffin Bay although at a 95 % confidence level with weak R^2 values (Fig. 4). Southerly, peripheral regions of the sea ice where the mean MO dates occur earliest, as described in Sect. 3, tend to have very weak R^2 relationships and insignificant trends, although the trend is negative for nearly all regions.

An interesting finding to note is the statistically significant (95 % confidence level) positive trend occurring in the Bering Sea. The Bering Sea is the only region of sea ice that shows a trend towards later MO dates through the data record. The relationship is weak (R^2 of 0.18) and the area of sea ice in the region is small ($2.7 \times 10^5 \text{ km}^2$), however, this region is showing an anomalous change in MO that is different from all other regions. Calculations for these trends and statistics are normalized to locations where MO dates exist in all years of the data record; however, the ice edge in this data set changes from year to year with the extent of sea ice at the beginning of March. Therefore it is interesting to note that the sea ice cover is actually more extensive in the Bering Sea in recent years than in the earliest years of the data record. For an example of this, see Fig. 1, where Bering Sea ice extent (using the 50 % concentration threshold) is greater in 2012 than in 1979.

The mean MO dates show a significant trend towards increasingly early MO for the majority of Arctic sea ice, in agreement with the works of others (e.g. Stroeve et al., 2006, 2014; Markus et al., 2009). Earlier MO on sea ice increases the amount of solar radiation that can be absorbed by the ice–ocean system by reducing surface albedo during the time of the year when solar radiation is greatest (Perovich et al., 2007). Increased absorption of solar radiation during the spring and can lead to increased heating in the Arctic, extensive loss of sea ice volume, and a delay in freeze-up following the melt season (Stroeve et al., 2014).

5 Summary

We have described an updated record of MO dates over Arctic sea ice that is now available for download from NSIDC (Anderson et al., 2014). This new data set utilizes the AHRA method for calculating the date of MO from passive microwave satellite data, which has improved consistency and been updated to include recent data from the SSMIS satellite sensor through 2012.

Based on this 34 year record of MO dates on Arctic sea ice we have shown that the timing of MO, on average, has some dependence on latitude. Typically, the sea ice periphery and southerly-located seas experience MO early in the year during the months of March and April, while northerly locations, in the central and western Arctic Ocean, experience MO in mid-late May. However, increased variability in regions within the Arctic Ocean shows that there is considerable year to year variability in MO timing which is attributed to variability in springtime weather conditions.

The 34 year record of MO dates shows significant, negative trends for the majority of the Arctic that indicate earlier MO. These trends in MO are on par with the warming trends observed in the Arctic over recent decades and the overall reduction of sea ice volume. However, the positive trend in the Bering Sea indicate the regional nature of MO timing and the need for more investigation into the variability of regional-scale atmospheric conditions surrounding the timing of MO.

The Supplement related to this article is available online at doi:10.5194/tcd-8-3037-2014-supplement.

Author Contribution

A. C. Bliss and M. R. Anderson collaborated on the ideas presented in this manuscript and in generation of data for Table 1 and Fig. 4. A. C. Bliss created Fig. 2 and wrote the initial draft of this manuscript with review and editing provided by M. R. Anderson.

Arctic sea ice melt onset from passive microwave satellite data: 1979–2012

A. C. Bliss and
M. R. Anderson

Title Page

Abstract

Introduction

Conclusions

References

Tables

Figures

◀

▶

◀

▶

Back

Close

Full Screen / Esc

Printer-friendly Version

Interactive Discussion



Acknowledgements. The Snow Melt Onset Over Arctic Sea Ice from SMMR and SSM/I-SSMIS Brightness Temperatures, Version 3 data set is available from NSIDC, Boulder, Colorado, USA (http://nsidc.org/data/docs/daac/nsidc0105_arctic_snowmelt_onset_dates.gd.html).

This work was supported by NASA MEaSUREs award NNX08AP34A. The authors thank W. Meier for providing regression coefficients used in the development of this data set and reviewers for their constructive comments.

References

- Abdalati, W., Steffen, K., Otto, C., and Jezek, K. C.: Comparison of brightness temperatures from SSM/I instruments on the DMSP F8 and F11 satellites for Antarctica and the Greenland Ice Sheet, *Int. J. Remote Sens.*, 16, 1223–1229, doi:10.1080/01431169508954473, 1995.
- Anderson, M. R. and Drobot, S. D.: Spatial and temporal variability in snowmelt onset over Arctic sea ice, *Ann. Glaciol.*, 33, 74–78, 2001.
- Anderson, M. R., Bliss, A. C., and Drobot, S. D.: Snow melt onset over Arctic sea ice from SMMR and SSM/I-SSMIS brightness temperatures, Version 3, 1979–2012, NASA DAAC at the National Snow and Ice Data Center, Boulder, Colorado, USA, available at: <http://nsidc.org/data/nsidc-0105.html>, last access: 2 June 2014.
- Belchansky, G. I., Douglas, D. C., and Platonov, N. G.: Duration of the Arctic sea ice melt season: regional and interannual variability 1979–2001, *J. Climate*, 17, 67–80, doi:10.1175/1520-0442(2004)017<0067:DOTASI>2.0.CO;2, 2004.
- Cavaliere, D., Parkinson, C., Gloersen, P., Comiso, J., and Zwally, H. J.: Deriving long-term time series of sea ice cover from satellite passive-microwave multisensor data sets, *J. Geophys. Res.*, 104, 15803–15814, doi:10.1029/1999JC900081, 1999.
- Curry, J. A., Schramm, J. L., and Ebert, E. E.: Sea ice-albedo climate feedback mechanism, *J. Climate*, 8, 240–247, doi:10.1175/1520-0442(1995)008<0240:SIACFM>2.0.CO;2, 1995.
- Drobot, S. D. and Anderson, M. R.: An improved method for determining snowmelt onset dates over Arctic sea ice using Scanning Multichannel Microwave Radiometer and Special Sensor Microwave/Imager data, *J. Geophys. Res.*, 106, 24033–24049, doi:10.1029/2000JD000171, 2001.

Arctic sea ice melt onset from passive microwave satellite data: 1979–2012

A. C. Bliss and
M. R. Anderson

Title Page

Abstract

Introduction

Conclusions

References

Tables

Figures

◀

▶

◀

▶

Back

Close

Full Screen / Esc

Printer-friendly Version

Interactive Discussion



Arctic sea ice melt onset from passive microwave satellite data: 1979–2012

A. C. Bliss and
M. R. Anderson

Title Page

Abstract

Introduction

Conclusions

References

Tables

Figures

◀

▶

◀

▶

Back

Close

Full Screen / Esc

Printer-friendly Version

Interactive Discussion



Forster, R. R., Long, D. G., Jezek, K. C., Drobot, S. D., and Anderson, M. R.: The onset of Arctic sea-ice snowmelt as detected with passive- and active-microwave remote sensing, *Ann. Glaciol.*, 33, 85–93, doi:10.3189/172756401781818428, 2001.

Jezek, K. C., Merry, C., Cavalieri, D., Grace, S., Bedner, J., Wilson, D., and Lampkin, D.: Comparison between SMMR and SSM/I Passive Microwave Data Collected over the Antarctic Ice Sheet, Byrd Polar Research Center Technical Report, no. 91-03, The Ohio State University, Columbus, Ohio, USA, 1991.

Kwok, R., Cunningham, G. F., and Nghiem, S. V.: A study of melt onset in RADARSAT SAR imagery, *J. Geophys. Res.*, 108, 3363, doi:10.1029/2002JC001363, 2003.

Kwok, R., Cunningham, G. F., Wensnahan, M., Rigor, I., Zwally, H. J., and Yi, D.: Thinning and volume loss of the Arctic Ocean sea ice cover: 2003–2008, *J. Geophys. Res.*, 114, C07005, doi:10.1029/2009JC005312, 2009.

Lindsay, R. W., Zhang, J., Schweiger, A., Steele, M., and Stern, H.: Arctic sea ice retreat in 2007 follows thinning trend, *J. Climate*, 22, 165–176, doi:10.1175/2008JCLI2521.1, 2009.

Markus, T., Stroeve, J. C., and Miller, J.: Recent changes in Arctic sea ice melt onset, freezeup, and melt season length, *J. Geophys. Res.*, 114, C12024, doi:10.1029/2009JC005436, 2009.

Maslanik, J., Drobot, S., Fowler, C., Emery, W., and Barry, R.: On the Arctic climate paradox and the continuing role of atmospheric circulation in affecting sea ice conditions, *Geophys. Res. Lett.*, 34, L03711, doi:10.1029/2006GL028269, 2007.

Maslanik, J., Stroeve, J., Fowler, C., and Emery, W.: Distribution and trends in Arctic sea ice age through spring 2011, *Geophys. Res. Lett.*, 38, L13502, doi:10.1029/2011GL047735, 2011.

Meier, W. N., Stroeve, J., and Fetterer, F.: Wither Arctic sea ice? A clear signal of decline regionally, seasonally and extending beyond the satellite record, *Ann. Glaciol.*, 46, 428–434, doi:10.3189/172756407782871170, 2007.

Meier, W. N., Fetterer, F., Savoie, M., Mallory, S., Duerr, R., and Stroeve, J.: NOAA/NSIDC Climate Data Record of Passive Microwave Sea Ice Concentration, Version 2, National Snow and Ice Data Center, Boulder, Colorado, USA, doi:10.7265/N55M63M1, 2013.

Nghiem, S. V., Rigor, I. G., Perovich, D. K., Clemente-Colón, P., Weatherly, J. W., and Neumann, G.: Rapid reduction of Arctic perennial sea ice, *Geophys. Res. Lett.*, 34, L19504, doi:10.1029/2007GL031138, 2007.

Parkinson, C. L. and Comiso, J. C.: On the 2012 record low Arctic sea ice cover: combined impact of preconditioning and an August storm, *Geophys. Res. Lett.*, 40, 1356–1361, doi:10.1002/grl.50349, 2013.

Arctic sea ice melt onset from passive microwave satellite data: 1979–2012

A. C. Bliss and
M. R. Anderson

Title Page

Abstract

Introduction

Conclusions

References

Tables

Figures

◀

▶

◀

▶

Back

Close

Full Screen / Esc

Printer-friendly Version

Interactive Discussion



Parkinson, C. L., Cavalieri, D. J., Gloersen, P., Zwally, H. J., and Comiso, J. C.: Arctic sea ice extents, areas, and trends, 1978–1996, *J. Geophys. Res.*, 104, 20837–20856, doi:10.1029/1999JC900082, 1999.

Perovich, D. K., Nghiem, S. V., Markus, T., and Schweiger, A.: Seasonal evolution and inter-annual variability of the local solar energy absorbed by the Arctic sea ice–ocean system, *J. Geophys. Res.*, 112, C03005, doi:10.1029/2006JC003558, 2007.

Smith, D. M.: Observation of perennial Arctic sea ice melt and freeze-up using passive microwave data, *J. Geophys. Res.*, 103, 27753–27769, doi:10.1029/98JC02416, 1998.

Stroeve, J. C., Maslanik, J., and Xiaoming, L.: An intercomparison of DMSP F11- and F13-derived sea ice products, *Remote Sens. Environ.*, 64, 132–152, doi:10.1016/S0034-4257(97)00174-0, 1998.

Stroeve, J. C., Markus, T., Meier, W., and Miller, J.: Recent changes in the Arctic melt season, *Ann. Glaciol.*, 44, 367–374, doi:10.3189/172756406781811583, 2006.

Stroeve, J. C., Markus, T., Boisvert, L., Miller, J., and Barrett, A.: Changes in Arctic melt season and implications for sea ice loss, *Geophys. Res. Lett.*, 41, 1216–1225, doi:10.1002/2013GL058951, 2014.

Wang, L., Wolken, G. J., Sharp, M. J., Howell, S. E. L., Derksen, C., Brown, R. D., Markus, T., and Cole, J.: Integrated pan-Arctic melt onset detection from satellite active and passive microwave measurements, 2000–2009, *J. Geophys. Res.*, 116, D22103, doi:10.1029/2011JD016256, 2011.

Winebrenner, D. P., Nelson, E. D., Colony, R., and West, R. D.: Observation of melt onset on multiyear Arctic sea ice using the ERS-1 synthetic aperture radar, *J. Geophys. Res.*, 99, 22425–22441, doi:10.1029/94JC01268, 1994.

Arctic sea ice melt onset from passive microwave satellite data: 1979–2012

A. C. Bliss and
M. R. Anderson

Table 1. Mean regional melt onset date statistics for 1979–2012.

	Region Area (10 ⁵ km ²)	Mean MO date (DOY)	Mean Standard Deviation (days)	Mean Earliest MO (DOY)	Mean Latest MO (DOY)	Mean Range (days)
Arctic Region	110.0	13 May (132.5)	7.3	121.0	146.5	25.5
Barents Sea	3.5	4 Apr (93.9)	12.2	69.5	121.8	52.2
Kara Sea	8.3	11 May (130.5)	12.8	98.4	152.4	54.0
Laptev Sea	8.4	25 May (144.9)	11.7	115.9	167.1	51.2
East Siberian Sea	12.6	31 May (150.1)	14.5	127.4	174.8	47.4
Chukchi Sea	8.2	17 May (136.3)	12.7	112.6	160.6	48.0
Beaufort Sea	9.0	28 May (148.0)	9.9	130.1	165.3	35.2
Canadian Archipelago	7.4	29 May (149.0)	7.7	135.9	168.2	32.2
Central Arctic	17.9	10 Jun (160.9)	9.5	143.8	181.5	37.7
Sea of Okhotsk	6.3	22 Mar (80.8)	5.3	70.9	93.3	22.4
Bering Sea	2.7	21 Mar (79.9)	7.2	69.8	95.7	25.9
Hudson Bay	13.3	17 Apr (106.6)	8.6	89.2	125.0	35.8
Baffin Bay	8.2	1 May (120.6)	10.0	102.5	137.7	35.2
Greenland Sea	4.0	29 Apr (118.9)	11.1	96.3	135.0	38.7
Baltic Sea	0.2	20 Mar (78.8)	10.4	63.0	99.4	36.4
St. Lawrence Gulf	0.1	15 Mar (73.2)	6.4	62.1	91.6	29.4

Title Page

Abstract

Introduction

Conclusions

References

Tables

Figures

◀

▶

◀

▶

Back

Close

Full Screen / Esc

Printer-friendly Version

Interactive Discussion

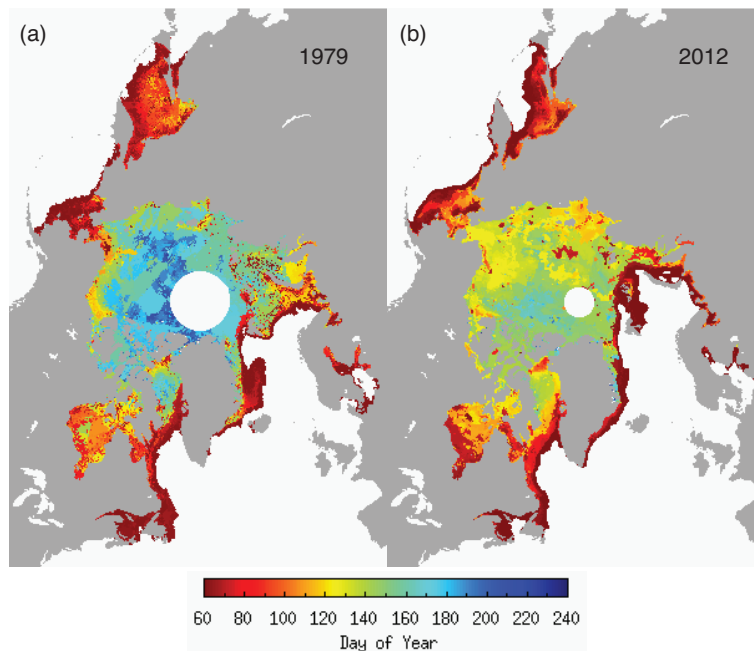
Arctic sea ice melt onset from passive microwave satellite data: 1979–2012A. C. Bliss and
M. R. Anderson

Figure 1. Annual melt onset date maps for **(a)** 1979 and **(b)** 2012 (maps available from Anderson et al., 2014).

[Title Page](#)[Abstract](#)[Introduction](#)[Conclusions](#)[References](#)[Tables](#)[Figures](#)[◀](#)[▶](#)[◀](#)[▶](#)[Back](#)[Close](#)[Full Screen / Esc](#)[Printer-friendly Version](#)[Interactive Discussion](#)



Figure 2. Melt onset date region map.

Arctic sea ice melt onset from passive microwave satellite data: 1979–2012

A. C. Bliss and
M. R. Anderson

Title Page	
Abstract	Introduction
Conclusions	References
Tables	Figures
◀	▶
◀	▶
Back	Close
Full Screen / Esc	
Printer-friendly Version	
Interactive Discussion	



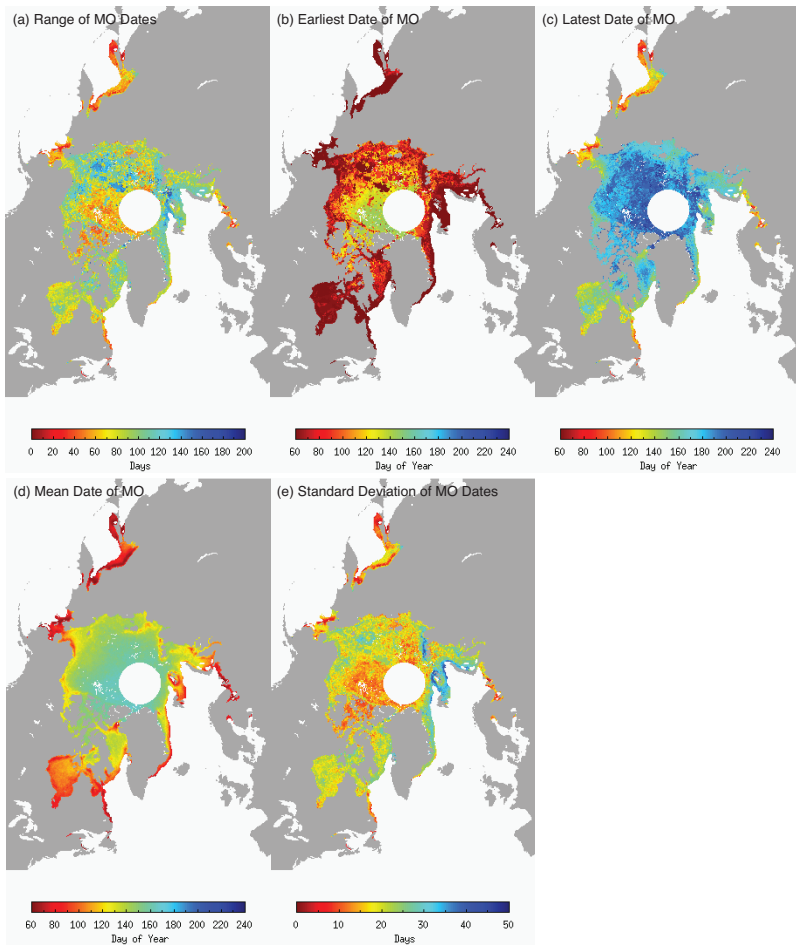


Figure 3. (a) Earliest, (b) latest, (c) range, (d) mean, and (e) standard deviation of melt onset dates for the 1979–2012 record (maps available from Anderson et al., 2014).

Arctic sea ice melt onset from passive microwave satellite data: 1979–2012

A. C. Bliss and
M. R. Anderson

Title Page

Abstract

Introduction

Conclusions

References

Tables

Figures

◀

▶

◀

▶

Back

Close

Full Screen / Esc

Printer-friendly Version

Interactive Discussion



Arctic sea ice melt onset from passive microwave satellite data: 1979–2012

A. C. Bliss and
M. R. Anderson

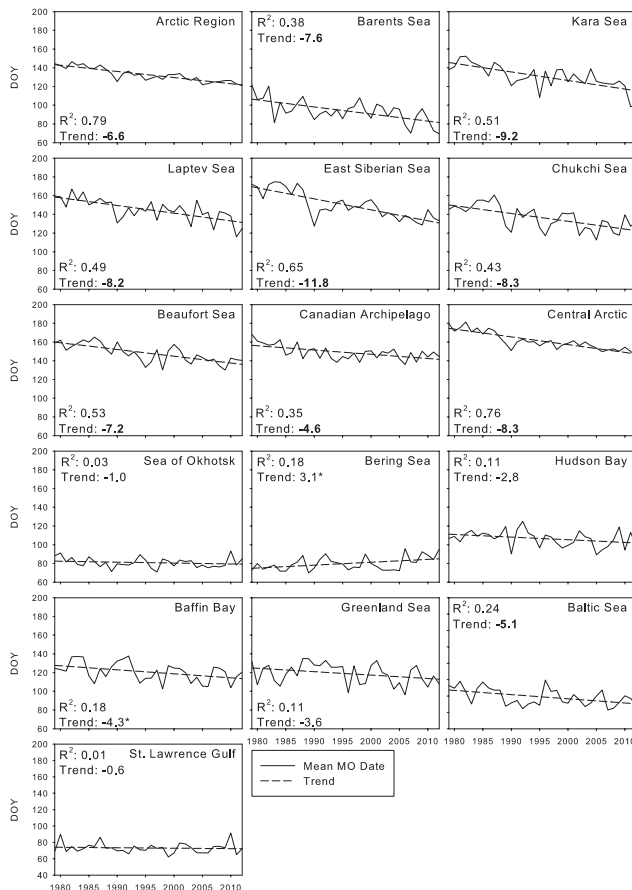


Figure 4. Time series of annual mean MO date and least squares linear regression trend for the Arctic Region and sub-regions. The R^2 value and decadal trend (days decade⁻¹) are shown for each region. Bold trends are statistically significant at a 99 % confidence level. An * indicates statistically significant trends at a 95 % confidence level.

Title Page

Abstract Introduction

Conclusions References

Tables Figures

◀ ▶

◀ ▶

Back Close

Full Screen / Esc

Printer-friendly Version

Interactive Discussion

